[13] Solution Structure and Dynamics of Integral Membrane Proteins by NMR: A Case Study Involving the Enzyme PagP

By PETER M. HWANG and LEWIS E. KAY

Abstract

Solution NMR spectroscopy is rapidly becoming an important technique for the study of membrane protein structure and dynamics. NMR experiments on large perdeuterated proteins typically exploit the favorable relaxation properties of backbone amide ^{15}N–^{1}H groups to obtain sequence-specific chemical shift assignments, structural restraints, and a wide range of dynamics information. These methods have proven successful in the study of the outer membrane enzyme, PagP, not only for obtaining the global fold of the protein but also for characterizing in detail the conformational fluctuations that are critical to its activity. NMR methods can also be extended to take advantage of slowly relaxing methyl groups, providing additional probes of structure and dynamics at side chain positions. The current work on PagP demonstrates how solution NMR can provide a unique atomic resolution description of the dynamic processes that are key to the function of many membrane protein systems.

Introduction

Propelled by recent methodological advances, the first detailed studies of membrane proteins by solution state nuclear magnetic resonance (NMR) spectroscopy are beginning to emerge. To date, four multispan structures have been determined including the glycophorin A helical dimer (MacKenzie *et al*., 1997) and the β-barrels, OmpX (Fernandez *et al*., 2001), OmpA (Arora *et al*., 2001), and PagP (Hwang *et al*., 2002). Significant progress has also been made in characterizing diacylglycerol kinase, as reviewed in this issue. This chapter highlights the techniques used to study PagP and how these can be further extended and applied to membrane proteins in general.

PagP is a 161-residue outer membrane enzyme found in a number of pathogenic Gram-negative bacteria (Hwang *et al*., 2002) that catalyzes the transfer of palmitate from phospholipids to lipopolysaccharide (LPS) (Bishop *et al*., 2000), the main lipid component of the outer membrane outer leaflet. As such, LPS forms an important barrier against host

0076-6879/05 $35.00

defenses, and PagP activity has been found to be essential for virulence in some microorganisms (Guo *et al*., 1998; Preston *et al*., 2003; Robey *et al*., 2001). The protein is ideal for study by NMR because of its small size, unique enzymatic activity, and biological significance.

Sample Preparation

For all but the smallest of membrane protein systems (<30 kDa total), a ^{2}H, ^{13}C, ^{15}N-enriched sample is required for the multidimensional NMR experiments used to obtain chemical shift assignments. Due to the high cost associated with isotope labeling, a rigorous optimization of protein production and sample preparation is warranted. Fortunately, ^{15}N enrichment alone is sufficient for screening purposes, and we have found that ^{1}H–^{15}N heteronuclear single-quantum correlation (HSQC) spectra recorded on protonated systems with a total molecular weight as large as 100 kDa are still useful for assessing feasibility.

Membrane proteins are notoriously difficult to overexpress. In *Escherichia coli*, however, some membrane proteins can be engineered to aggregate in an unfolded form, so that they do not interfere with cell viability and are not susceptible to degradation. While such strategies can enhance yields by at least an order of magnitude, they do require effective protocols for reconstituting the inactive protein. Very few successful examples of this methodology have been reported for helical membrane proteins (Booth, 2003; Kiefer, 2003), but the approach has become relatively routine for β-barrels (Bannwarth and Schulz, 2003; Buchanan, 1999), a rare class of membrane proteins found only in the outer membranes of Gram-negative bacteria, mitochondria, and chloroplasts. Like other β-barrels, PagP could be made to accumulate in a dense unfolded form ($\sim$30 mg/liter of culture) by removing its N-terminal signal sequence (Nielsen *et al*., 1997) via mutagenesis. Denatured PagP has been successfully reconstituted into DPC, OG/SDS, and CYFOS-7 detergents (Fig. 1), and NMR spectra indicate a similarly folded structure in all three environments, although there are some important differences (see below).

The selection of an appropriate detergent (or lipid) is, of course, key to a successful refolding strategy, but detergents must also be screened for their ability to maintain protein structure and for suitability in NMR studies (Krueger-Koplin *et al*., 2004). Anionic detergents like sodium dodecyl sulfate (SDS) and perfluorooctonate (PFO) form small micelles, but these totally denature PagP (Fig. 2). On the other hand, solublization in nonionic detergents like octylglucoside (OG) and dodecylmaltoside (DM) tend to produce samples that give very broad NMR signals. Zwitterionic

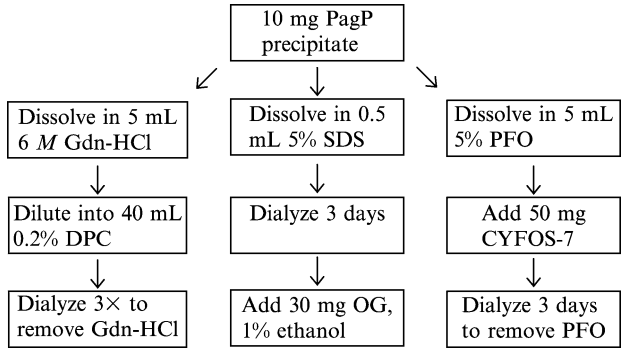

FIG. 1. Flow chart of three alternative folding protocols for PagP. In all cases, the buffer is 50 m*M* sodium phosphate, pH 6.0.

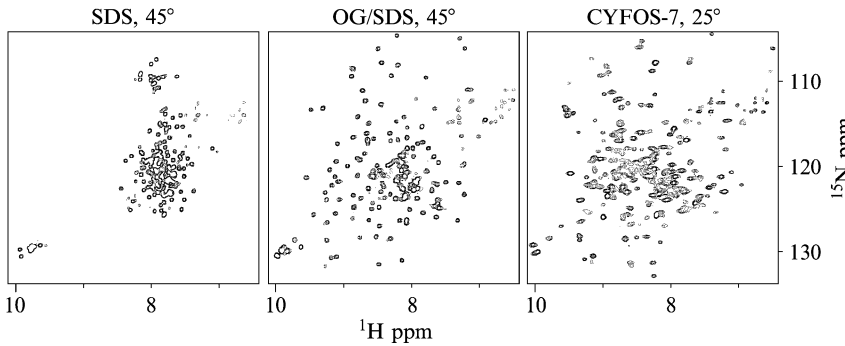

FIG. 2. ^{1}H–^{15}N HSQC spectra of 1 m*M* ^{2}H, ^{15}N-PagP samples, 50 m*M* sodium phosphate, pH 6.0, in three different detergent environments: SDS, OG/SDS, and CYFOS-7.

detergents like dodecylphosphocholine (DPC) and dihexanoylphosphatidylcholine (DHPC) provide a good compromise between micelle size and protein stability. For proteins that are particularly difficult to work with, an important advance is the development of lipopeptide detergents (LPDs) (McGregor *et al.*, 2003). LPDs form small micelles, yet they are able to maintain the activity of ''fragile'' proteins like lactose permease longer than DM. Excellent NMR spectra of PagP in LPD have been obtained, with the rotational correlation time of the complex comparable to that of PagP–DPC and PagP–OG/SDS (McGregor *et al.*, 2003).

Chemical Shift Assignment

Obtaining chemical shift assignments is the first step toward characterizing any system by NMR. In applications to high-molecular-weight proteins where deuteration is critical, the key assignment experiments center around the backbone amide ^{15}N–^{1}H group. The use of TROSY (Pervushin *et al.*, 1997) is essential in large systems like PagP (50–60 kDa in total), because it minimizes transverse relaxation of amide ^{15}N and ^{1}H spins leading to substantial improvements in the sensitivity and resolution of out-and-back experiments like the HNCA, HN(CO)CA, HN(CA)CB, HN(COCA)CB, HN(CA)CO, and HNCO (Salzmann *et al.*, 1998; Yang and Kay, 1999). Using these TROSY-modified sequences, >90% of the backbone resonances could be assigned in PagP in both DPC and OG/SDS detergents (Hwang *et al.*, 2002), and the only regions of the protein that could not be assigned were those broadened beyond detection by conformational exchange.

N–H groups are key probes for obtaining atomic level structural and dynamic information, provided that protons can be efficiently incorporated into these sites (in an otherwise deuterated background) and sequence-specific assignments are available. In PagP, incorporating protons at backbone amide positions via solvent exchange is straightforward because the protein is purified from an unfolded state. In addition to protonation at backbone amide sites, it is also possible to incorporate protons into methyl groups of Val, Leu, and Ile ($\delta 1$ only) using ^{2}H,^{13}C, ^{1}H-methyl-labeled precursors, α-ketoisovalerate, and α-ketobutyrate, in *E. coli*–based growths (Gardner and Kay, 1998; Goto *et al.*, 1999). The methyl ^{13}C,^{1}H chemical shifts can be assigned by relaying magnetization to backbone N–H groups using experiments that are specifically optimized for methyl protonated, highly deuterated proteins (Gardner *et al.*, 1996; Hilty *et al.*, 2002); however the sensitivity of these experiments can be quite low for large systems. Recently new experiments for application to high-molecular-weight proteins have been developed that make use of COSY-type relays to correlate methyl groups with backbone amides, aliphatic side chain, or backbone CO carbons, significantly improving sensitivity (Tugarinov and Kay, 2003). For Val and Leu residues, these schemes require an alternate labeling strategy in which one of the methyls in a given residue is $^{13}C^{1}H_3$ labeled and the other $^{12}C^{2}H_3$, achieving a linear ^{13}C aliphatic side chain spin system.

Structure Determination

Structural studies of OmpX (Fernandez *et al.*, 2001), OmpA (Arora *et al.*, 2001), and PagP (Hwang *et al.*, 2002) were greatly facilitated by the β-barrel architecture of these proteins, with amide NOEs connecting

proximal strands. Combined with hydrogen bond restraints and chemical shift–based dihedral angle restraints (Cornilescu *et al*., 1999; Wishart and Case, 2001), a reasonably high-resolution global fold (<1.0 Å RMSD for the backbone heavy atoms of the β-barrel) could be obtained for PagP solublized in either DPC (Fig. 3) or in OG/SDS. The overall structure of PagP in both environments is essentially the same, indicating that the type of solubilizing detergent used and the nature of the reconstitution procedure do not strongly perturb the global fold of this enzyme. A recently determined X-ray crystal structure of PagP in LDAO (unpublished observations) is also in close agreement with the NMR-derived structures.

For most soluble proteins, NH–NH NOEs alone would be insufficient for the establishment of a global fold (Gardner *et al*., 1997), but in β-barrels, inter-strand NOEs between amides are very effective in defining the barrel topology (Fig. 4). However, the positioning of elements outside the PagP β-barrel, including the orientation of loops and the amphipathic α-helix, is poorly defined by NH–NH NOEs alone. The X-ray structure of PagP in LDAO indicates that most of these components are well structured, with the α-helix packing against strands B and C. (A careful analysis of the relative positions of the amphipathic helix and aromatic side chains, based on the crystal structure, has shown that PagP is tilted by 30° relative to the bilayer normal, the first example of a tilted β-barrel membrane protein.) One clear way of improving the quality of NMR-derived

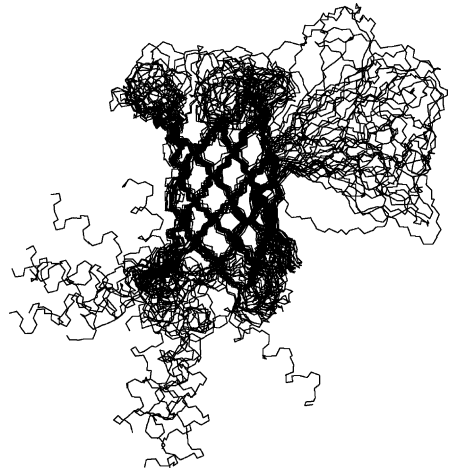

FIG. 3. Superposition of 20 NMR structures of PagP in DPC. Adapted from Hwang *et al.* (2002). Copyright 2002 National Academy of Sciences, USA.

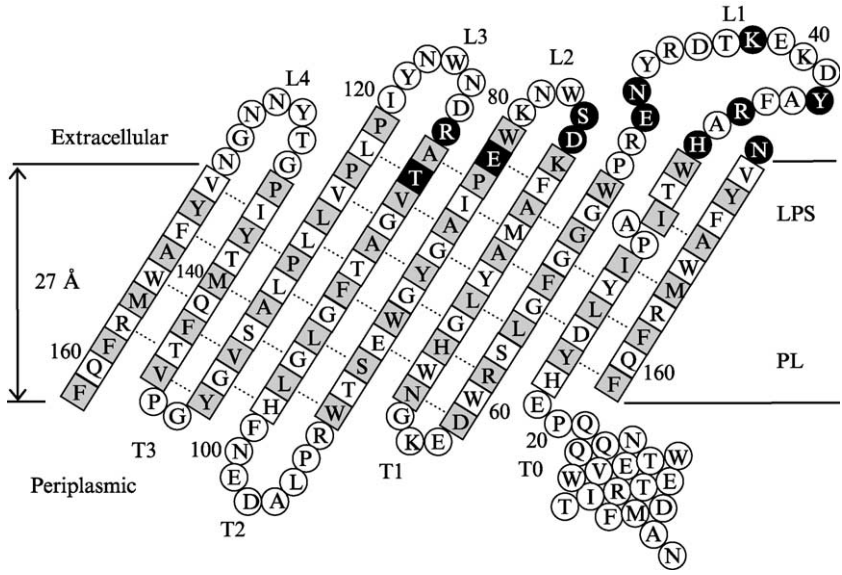

FIG. 4. Topology diagram of PagP. Residues in a β-sheet conformation are represented as squares, and all others as circles. Gray-shaded and nonshaded squares denote those residues with side chains pointing toward the exterior or interior of the β-barrel, respectively. Absolutely conserved polar residues in the extracellular region of the protein (putative active site) are shown in black. Slowly exchanging amides, as detected by ^{1}H–^{15}N HSQC spectra recorded on a D_2O-exchanged sample of PagP–OG/SDS, are indicated by dotted lines between hydrogen bonding partners. Adapted from Hwang *et al.* (2002). Copyright 2002 National Academy of Sciences, USA.

structures is to include NH–CH_3 and CH_3–CH_3 NOEs (Mueller *et al.*, 2000), using the methyl-labeling scheme described above. Methyl NOEs have been shown to improve the accuracy and precision of NMR-derived structures for OmpX (Fernandez *et al.*, 2004), and they would be indispensable for defining helix packing and global folds of α-helical proteins. Another important source of structural information comes from residual dipolar couplings (Prestegard, 1998; Tjandra and Bax, 1997). Unfortunately, most alignment media are incompatible with the detergents used to solubilize membrane proteins (Ma and Opella, 2000). Strain-induced alignment in a gel (Ishii *et al.*, 2001; Sass *et al.*, 2000) has been used to align PagP in DPC micelles. However, the polyacrylamide matrix significantly reduces the effective concentration of the protein, limiting sensitivity. Clearly other alignment strategies must be explored.

Dynamics

Backbone amide ^{15}N and side chain methyl ^{13}C spins are excellent probes of molecular dynamics covering a wide range of time scales. Although this chapter will focus on applications involving backbone amide groups, it is worthwhile to note that methods similar to those for ^{15}N–^{1}H spin systems have been developed to study dynamics using methyl groups. For instance, the relaxation of methyl groups can be optimized using methyl-TROSY (Tugarinov *et al.*, 2003), leading to a CPMG-based multiple quantum relaxation dispersion experiment (Korzhnev *et al.*, 2004) that has been used to characterize conformational exchange in the 82-kDa protein, malate synthase G.

^{15}N T_1, T_2, and heteronuclear ^{1}H-^{15}N NOE measurements are routinely performed on water-soluble proteins (Bruschweiler, 2003), and recently such experiments have also been applied to OmpX (Fernandez *et al.*, 2004), OmpA (Tamm *et al.*, 2003), and PagP (Hwang *et al.*, 2002). Each of those proteins shows a large diversity in the amplitudes of amide bond vector dynamics (on a picosecond to nanosecond time scale). In PagP, T_1 relaxation times are a sensitive indicator of nanosecond motions, identifying three different regions with high mobility on this time scale (Fig. 5). T_2 relaxation times and heteronuclear NOE values show pronounced differences from mean values at the very N-terminus (first few residues prior to the α-helix) and in the large L1 extracellular loop, indicating that these

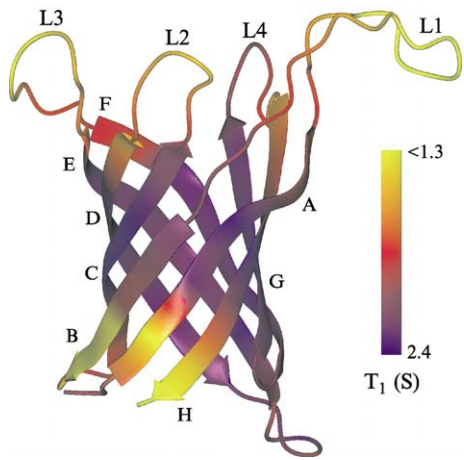

FIG. 5. Ribbon diagram of the PagP β-barrel colored according to measured T_1 times in DPC at 45°. Residues for which T_1 times could not be measured were assigned values midway between flanking residues.

regions are the most flexible in the protein (picosecond time scale). Notably, these elements were not observed in the X-ray structure of PagP in LDAO. Many putative active site residues are located in the L1 loop (see Fig. 4), suggesting that it must rigidify considerably for catalysis to occur. It is clear that attempts to understand how this enzyme functions must go significantly beyond static structure determination.

Although the active site of PagP could not be visualized in NMR or X-ray-derived structures, the crystal structure did establish the presence of a single inhibitory LDAO detergent molecule buried in the large central cavity of the barrel. This suggests that the active site of the enzyme is inside the β-barrel, and this finding is supported by a subsequent mutagenesis study (unpublished observations). Since it is probable that many linear chain detergents can also fit inside the barrel, inhibiting enzyme activity, we chose to refold PagP into a new detergent, CYFOS-7, which is similar to DPC except that it possesses a bulky cyclohexyl ring at the terminus of its alkyl chain that prevents entry into the barrel. PagP was found to retain catalytic activity in CYFOS-7 (unpublished observations), unlike all the other detergents that had been used for previous structural studies. With a functioning system in hand we now focus on how phospholipid substrate might diffuse into the barrel and attempt to characterize the dynamic features of the enzyme that are important for activity.

At 45° the ^{1}H–^{15}N HSQC spectrum of PagP in CYFOS-7 resembles that of PagP–DPC and PagP–OG/SDS, suggesting a similar structure in all three environments. However, at 25° the spectrum changes dramatically, with an approximate doubling of peaks (see Fig. 2). Backbone chemical shift assignments establish the presence of a second state, with a fractional population of approximately 0.3. The major ''R'' form is similar to the conformers observed in other detergents, but the new ''T'' state possesses very distinct chemical shifts (Fig. 6), suggesting a complete restructuring of the ''β-bulge'' of strand A and an ordering of the L1 loop. It is not unusual for membrane proteins to adopt multiple conformations, as can be seen from the wide range of structures that are crystallized within a single class of proteins (Chang, 2003; Jiang *et al*., 2002). The major advantage of using NMR to probe membrane proteins is that they can be studied in their functionally active forms and processes involving the interconversion between states can be monitored directly, as in the case of PagP in CYFOS-7 (unpublished observations), described below.

The relative populations of R and T states can be measured directly from peak volumes in HSQC spectra. However, relaxation losses during the pulse sequence must be carefully accounted for, since the two conformers have very different relaxation properties. An unenhanced HSQC pulse scheme was employed, with ^{15}N TROSY component selection

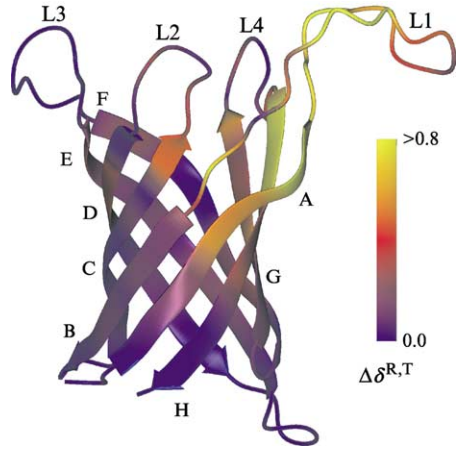

FIG. 6. Ribbon diagram of the PagP β-barrel colored according to the combined chemical shift difference between the R and T states, $\Delta\delta^{R,T} = [(\omega_N\Delta\delta_N)^2 + (\omega_{C\alpha}\Delta\delta_{C\alpha})^2 + (\omega_{CO}\Delta\delta_{CO})^2]^{1/2}, \omega_N = 0.154, \omega_{C\alpha} = 0.276, \omega_{CO} = 0.341$ (Evenas *et al.*, 2001). For the R state, an average of the available chemical shifts in DPC, OG/SDS, and the CYFOS-7 R state was used. If a residue could not be observed in the T state (mainly loop L3) or if the R and T states were identical, $\Delta\delta^{R,T} = 0$. Adapted from Hwang *et al.* (2004). Copyright 2004 National Academy of Sciences, USA.

achieved using the IPAP procedure (Ottiger *et al.*, 1998; Yang and Nagayama, 1996). In this way relaxation losses could be easily taken into account by considering only the decay of single quantum ^{1}H and ^{15}N magnetization. Equilibrium constants were obtained for the R,T interconversion over a temperature range from 15° to 35°, and from the linear plot of ln K_{eq} vs. inverse temperature, values of $\Delta H = 10.7$ kcal/mol and $\Delta S = 37.5$ cal/mol/K were calculated for the T-to-R transition.

Kinetic rate constants describing the exchange between R and T states can also be obtained from solution NMR studies. In theory, a NOESY-type experiment could be employed to measure exchange-mediated transfer of proton magnetization (Montelione and Wagner, 1989). However, a better alternative is the N_{ZZ} exchange experiment, in which magnetization is stored as N_Z during the mixing time rather than as H_Z. In this simple 2D experiment, evolution of ^{15}N chemical shift occurs prior to the exchange of magnetization between sites so that cross-peaks at (ω_N^A, ω_H^B) and (ω_N^B, ω_H^A) are obtained, in addition to diagonal peaks at (ω_N^A, ω_H^A) and (ω_N^B, ω_H^B). The original N_{ZZ} exchange experiment (Farrow *et al.*, 1994) was modified to select for the ^{15}N TROSY component using the IPAP approach (Fig. 7). Rate constants, $k_{RT} = 2.8\ s^{-1}$ and $k_{TR} = 6.5\ s^{-1}$, for the R,T interconversion at 25° were extracted from simultaneous fits of the decay/buildup of

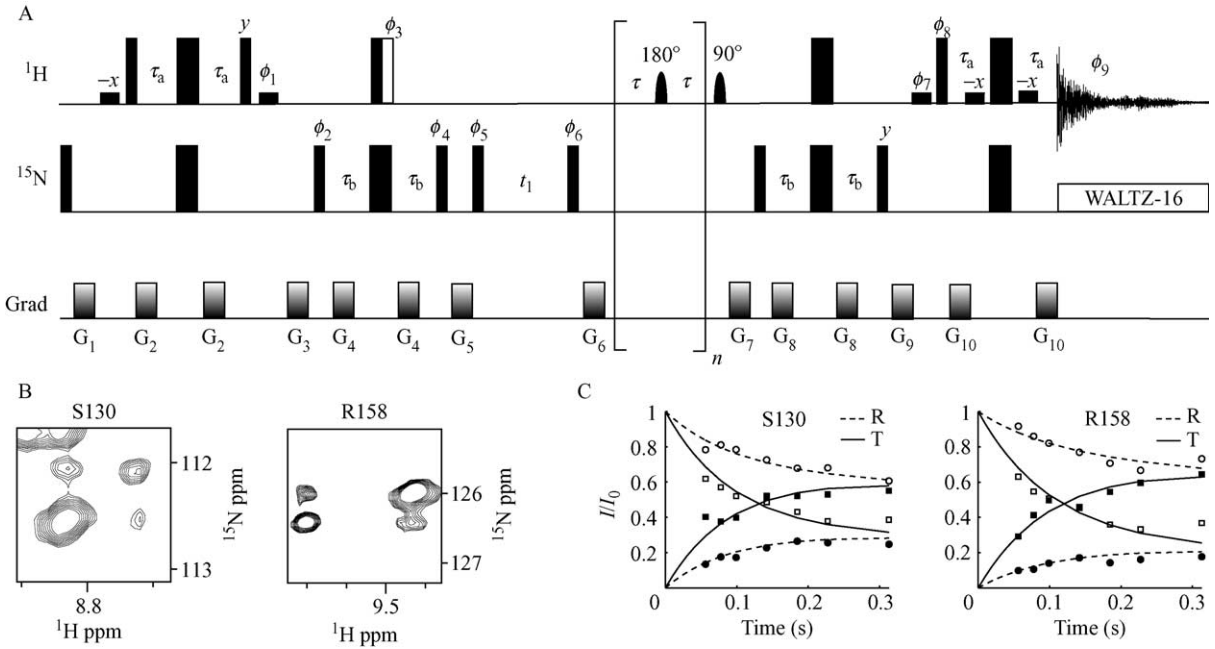

FIG. 7. (A) Pulse sequence of the IPAP-N_{zz} exchange experiment. The ^{1}H and ^{15}N carriers are positioned at 4.78 (water) and 119 ppm, respectively. All narrow (wide) rectangles denote nonselective 90° (180°) pulses along the x-axis, unless otherwise specified. The shaped (RE-BURP) 180° pulse during the mixing time (in brackets) is selective for the amide region to remove cross-correlation/cross-relaxation effects. The shaped 90° pulse after the mixing time selectively excites the upfield aliphatic region, to eliminate detergent signal that has recovered during the mixing time. The delays used are $\tau_a = 2.3$ ms, $\tau_b = 2.75$ ms, and $\tau = 10$ ms. To record a spectrum in which the ^{15}N doublets are antiphase, the phase cycle is as follows: $\phi_1 = y$; $\phi_2 = 4(x), 4(-x)$; $\phi_3 = -x$; $\phi_4 = x$; $\phi_5 = x, -x$; $\phi_6 = 2(-x), 2(x)$, $\phi_7 = -x, x$; $\phi_8 = -x, x$; and $\phi_9 = (x, x, -x, -x, -x, -x, x, x)$. For in-phase selection, the phase cycle is

diagonal/cross-peaks as a function of mixing time to a model that accounts for longitudinal ^{15}N T_1 relaxation and a single exchange process (Tollinger *et al.*, 2001).

At temperatures below approximately 35°, both R and T forms of PagP give rise to correlations in HSQC spectra, and it is relatively easy, therefore, to quantify the exchange process using magnetization transfer experiments. At higher temperatures, where only a single set of peaks corresponding to the R state is observed, a different approach must be used. In principle, the kinetics of interconversion, the relative populations of the interconverting states, and chemical shift differences, $\Delta\omega$, between conformers for individual residues can be extracted from CPMG-based relaxation dispersion experiments, as reviewed in detail elsewhere (Palmer *et al.*, 2001). In the case of PagP at 45°, the largest dispersions were well fit individually with similar time constants, suggesting that these profiles report on the same process. All of the dispersion data were subsequently fit to a single global exchange process (Mulder *et al.*, 2001), with $\Delta\omega$ varied for each residue. The fitted $\Delta\omega$ values at 45° correlate well with those measured directly in spectra recorded at 25°, suggesting that the dominant exchange process at this temperature is the R,T interconversion, with rate constants of $k_{RT} = 33\ s^{-1}$ and $k_{TR} = 298\ s^{-1}$.

As described above, positive values of ΔH and ΔS are extracted for the T-to-R transition, consistent with a local unfolding reaction in which the L1 loop and portions of strands A and H (Fig. 6) become more dynamic. The increased dynamics in the R state are quite apparent from a simple ^{1}H–^{15}N HSQC spectrum recorded at 25°, where correlations from the R conformer are significantly broadened relative to the corresponding cross-peaks from the T-state (Fig. 8A). While dispersion curves for residues in the T state can be fit to a slow process matching the T-to-R transition (6.5 s^{-1}), fits of dispersions derived from residues in the R state suggest additional exchange processes that are much faster ($\sim 10^3\ s^{-1}$) than the R-to-T conversion (2.8 s^{-1}) (Fig. 8B). Thus, a picture emerges in which

the same, except that $\phi_1 = -y$, $\phi_3 = x$, and $\phi_4 = y$. Addition or subtraction of the in-phase and antiphase spectra yields the ^{15}N TROSY or anti-TROSY component. Quadrature detection in F_1 is achieved by States-TPPI (Marion *et al.*, 1989) of ϕ_5. The duration and strength of the gradients are as follows: G_1 = (1 ms, 5 G/cm); G_2 = (0.2 ms, 8 G/cm); G_3 = (0.5 ms, 12 G/cm); G_4 = (0.25 ms, 10 G/cm); G_5 = (0.4 ms, 5 G/cm); G_6 = (0.3 ms, 15 G/cm); G_7 = (0.2 ms, 7 G/cm); G_8 = (0.3 ms, 8 G/cm); G_9 = (0.25 ms, 10 G/cm); G_{10} = (0.3 ms, 15 G/cm). (B) Region of a correlation map recorded with an IPAP-N_{zz} experiment showing diagonal and cross-peaks for S130 and R158. The largest peak in both panels corresponds to the diagonal peak of the R state. (C) Decay [correlations at (ω_N^A, ω_H^A); open symbols] and buildup [correlations at (ω_N^A, ω_H^B); closed symbols] curves for S130 and R158. The curves are normalized so that the intensities of the diagonal peaks (ω_N^A, ω_H^A) at time = 0 are 1.0 in both R and T states. Adapted from Hwang *et al.* (2004). Copyright 2004 National Academy of Sciences, USA.

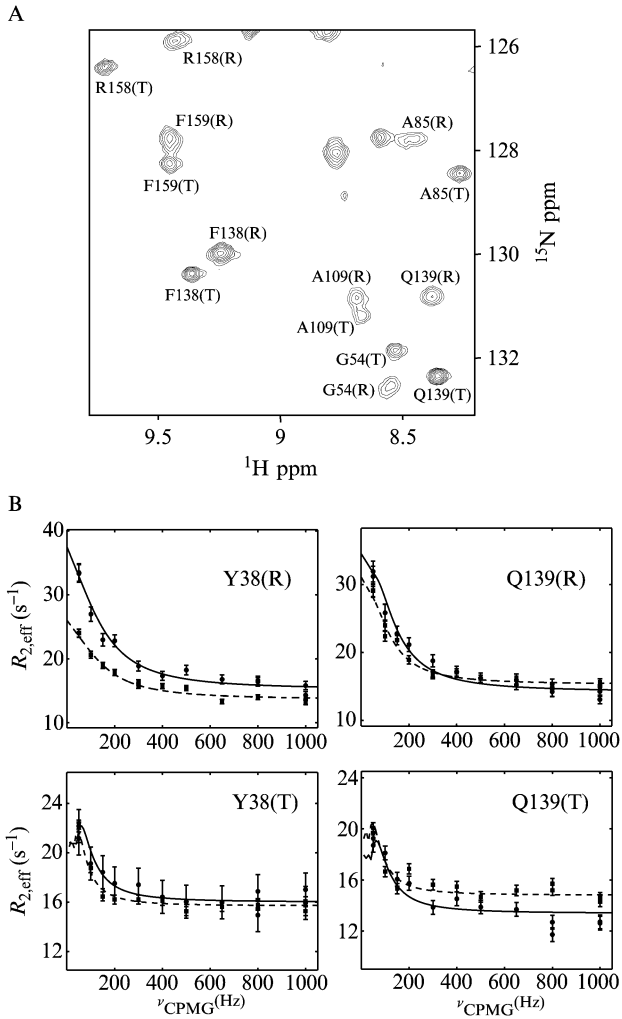

FIG. 8. (A) Selected region of the ^{1}H–^{15}N TROSY–HSQC spectrum of PagP–CYFOS-7 at 25°. (B) ^{15}N-CPMG relaxation dispersion curves for Y38 and Q139 in both R and T states at 25°, recorded at 800 (upper profile) and 600 MHz. $R_{2,\mathrm{eff}}$ is calculated as $-1/T_{\mathrm{CP}} \ln(I\nu_{\mathrm{cpmg}}/I_{\mathrm{o}})$, where T_{CP} is a 40 ms constant time CPMG element, and $I\nu_{\mathrm{cpmg}}$ and I_{o} are the intensities of correlations recorded in spectra with and without the T_{CP} period, respectively. T_{CP} is made up of (τ—^{15}N π pulse—τ) elements, where the effective RF field strength, ν_{CPMG}, equals $1/(4\tau)$ (Mulder *et al.*, 2002). Adapted from Hwang *et al.* (2004). Copyright 2004 National Academy of Sciences, USA.

the enhanced flexibility of the R state facilitates substrate entry into the central cavity, while the formation of a defined conformation of the peripheral L1 loop in the T state may lead to the production of a functional active site.

Conclusion

The significant structural rearrangements that occur during the R, T cycle in PagP demonstrate how a detailed description of dynamics is essential for an understanding of protein function. This is likely to be especially true of membrane proteins, which often depend on large conformational changes to regulate the transmission of solutes or signals across biological membranes. Solution NMR is thus ideally poised to make a significant and unique contribution to the structural biology of this important class of molecules.

References

Arora, A., Abildgaard, F., Bushweller, J. H., and Tamm, L. K. (2001). Structure of outer membrane protein A transmembrane domain by NMR spectroscopy. *Nat. Struct. Biol.* **8,** 334–338.

Bannwarth, M., and Schulz, G. E. (2003). The expression of outer membrane proteins for crystallization. *Biochim. Biophys. Acta* **1610,** 37–45.

Bishop, R. E., Gibbons, H. S., Guina, T., Trent, M. S., Miller, S. I., and Raetz, C. R. (2000). Transfer of palmitate from phospholipids to lipid A in outer membranes of Gram-negative bacteria. *EMBO J.* **19,** 5071–5080.

Booth, P. J. (2003). The trials and tribulations of membrane protein folding *in vitro*. *Biochim. Biophys. Acta* **1610,** 51–56.

Bruschweiler, R. (2003). New approaches to the dynamic interpretation and prediction of NMR relaxation data from proteins. *Curr. Opin. Struct. Biol.* **13,** 175–183.

Buchanan, S. K. (1999). Beta-barrel proteins from bacterial outer membranes: Structure, function and refolding. *Curr. Opin. Struct. Biol.* **9,** 455–461.

Chang, G. (2003). Structure of MsbA from Vibrio cholera: A multidrug resistance ABC transporter homolog in a closed conformation. *J. Mol. Biol.* **330,** 419–430.

Cornilescu, G., Delaglio, F., and Bax, A. (1999). Protein backbone angle restraints from searching a database for chemical shift and sequence homology. *J. Biomol. NMR* **13,** 289–302.

Evenas, J., Tugarinov, V., Skrynnikov, N. R., Goto, N. K., Muhandiram, R., and Kay, L. E. (2001). Ligand-induced structural changes to maltodextrin-binding protein as studied by solution NMR spectroscopy. *J. Mol. Biol.* **309,** 961–974.

Farrow, N. A., Zhang, O., Forman-Kay, J. D., and Kay, L. E. (1994). A heteronuclear correlation experiment for simultaneous determination of 15N longitudinal decay and chemical exchange rates of systems in slow equilibrium. *J. Biomol. NMR* **4,** 727–734.

Fernandez, C., Adeishvili, K., and Wuthrich, K. (2001). Transverse relaxation-optimized NMR spectroscopy with the outer membrane protein OmpX in dihexanoyl phosphatidylcholine micelles. *Proc. Natl. Acad. Sci. USA* **98,** 2358–2363.

Fernandez, C., Hilty, C., Wider, G., Guntert, P., and Wuthrich, K. (2004). NMR structure of the integral membrane protein OmpX. *J. Mol. Biol.* **336,** 1211–1221.

Gardner, K. H., and Kay, L. E. (1998). The use of 2H, 13C, 15N multidimensional NMR to study the structure and dynamics of proteins. *Annu. Rev. Biophys. Biomol. Struct.* **27,** 357–406.

Gardner, K. H., Konrat, R., Rosen, M. K., and Kay, L. E. (1996). An (H)C(CO)NH-TOCSY pulse scheme for sequential assignment of protonated methyl groups in otherwise deuterated N-15,C-13-labeled proteins. *J. Biomol. NMR* **8,** 351–356.

Gardner, K. H., Rosen, M. K., and Kay, L. E. (1997). Global folds of highly deuterated, methyl-protonated proteins by multidimensional NMR. *Biochemistry* **36,** 1389–1401.

Goto, N. K., Gardner, K. H., Mueller, G. A., Willis, R. C., and Kay, L. E. (1999). A robust and cost-effective method for the production of Val, Leu, Ile (delta 1) methyl-protonated 15N-, 13C-, 2H-labeled proteins. *J. Biomol. NMR* **13,** 369–374.

Guo, L., Lim, K. B., Poduje, C. M., Daniel, M., Gunn, J. S., Hackett, M., and Miller, S. I. (1998). Lipid A acylation and bacterial resistance against vertebrate antimicrobial peptides. *Cell* **95,** 189–198.

Hilty, C., Fernandez, C., Wider, G., and Wuthrich, K. (2002). Side chain NMR assignments in the membrane protein OmpX reconstituted in DHPC micelles. *J. Biomol. NMR* **23,** 289–301.

Hwang, P. M., Choy, W. Y., Lo, E. I., Chen, L., Forman-Kay, J. D., Raetz, C. R., Prive, G. G., Bishop, R. E., and Kay, L. E. (2002). Solution structure and dynamics of the outer membrane enzyme PagP by NMR. *Proc. Natl. Acad. Sci. USA* **99,** 13560–13565.

Hwang, P. M., Bishop, R. E., and Kay, L. E. (2004). The integral membrane enzyme PagP alternates between two dynamically distinct states. *Proc. Natl. Acad. Sci. USA* **101,** 9618–9623.

Ishii, Y., Markus, M. A., and Tycko, R. (2001). Controlling residual dipolar couplings in high-resolution NMR of proteins by strain induced alignment in a gel. *J. Biomol. NMR* **21,** 141–151.

Jiang, Y., Lee, A., Chen, J., Cadene, M., Chait, B. T., and MacKinnon, R. (2002). The open pore conformation of potassium channels. *Nature* **417,** 523–526.

Kiefer, H. (2003). *In vitro* folding of alpha-helical membrane proteins. *Biochim. Biophys. Acta* **1610,** 57–62.

Korzhnev, D. M., Kloiber, K., Kanelis, V., Tugarinov, V., and Kay, L. E. (2004). Probing slow dynamics in high molecular weight proteins by methyl-TROSY NMR spectroscopy: Application to a 723-residue enzyme. *J. Am. Chem. Soc.* **126,** 3964–3973.

Krueger-Koplin, R. D., Sorgen, P. L., Krueger-Koplin, S. T., Rivera-Torres, I. O., Cahill, S. M., Hicks, D. B., Grinius, L., Krulwich, T. A., and Girvin, M. E. (2004). An evaluation of detergents for NMR structural studies of membrane proteins. *J. Biomol. NMR* **28,** 43–57.

Ma, C., and Opella, S. J. (2000). Lanthanide ions bind specifically to an added ''EF-hand'' and orient a membrane protein in micelles for solution NMR spectroscopy. *J. Magn. Reson.* **146,** 381–384.

MacKenzie, K. R., Prestegard, J. H., and Engelman, D. M. (1997). A transmembrane helix dimer: Structure and implications. *Science* **276,** 131–133.

Marion, D., Ikura, M., Tschudin, R., and Bax, A. (1989). Rapid recording of 2D NMR-spectra without phase cycling—application to the study of hydrogen-exchange in proteins. *J. Magn. Reson.* **85,** 393–399.

McGregor, C. L., Chen, L., Pomroy, N. C., Hwang, P., Go, S., Chakrabartty, A., and Prive, G. G. (2003). Lipopeptide detergents designed for the structural study of membrane proteins. *Nat. Biotechnol.* **21,** 171–176.

Montelione, G. T., and Wagner, G. (1989). 2D chemical-exchange NMR-spectroscopy by proton-detected heteronuclear correlation. *J. Am. Chem. Soc.* **111,** 3096–3098.

Mueller, G. A., Choy, W. Y., Yang, D., Forman-Kay, J. D., Venters, R. A., and Kay, L. E. (2000). Global folds of proteins with low densities of NOEs using residual dipolar couplings: Application to the 370-residue maltodextrin-binding protein. *J. Mol. Biol.* **300,** 197–212.

Mulder, F. A., Mittermaier, A., Hon, B., Dahlquist, F. W., and Kay, L. E. (2001). Studying excited states of proteins by NMR spectroscopy. *Nat. Struct. Biol.* **8,** 932–935.

Mulder, F. A., Hon, B., Mittermaier, A., Dahlquist, F. W., and Kay, L. E. (2002). Slow internal dynamics in proteins: Application of NMR relaxation dispersion spectroscopy to methyl groups in a cavity mutant of T4 lysozyme. *J. Am. Chem. Soc.* **124,** 1443–1451.

Nielsen, H., Engelbrecht, J., Brunak, S., and von Heijne, G. (1997). Identification of prokaryotic and eukaryotic signal peptides and prediction of their cleavage sites. *Protein Eng.* **10,** 1–6.

Ottiger, M., Delaglio, F., and Bax, A. (1998). Measurement of J and dipolar couplings from simplified two-dimensional NMR spectra. *J. Magn. Reson.* **131,** 373–378.

Palmer, A. G., 3rd, Kroenke, C. D., and Loria, J. P. (2001). Nuclear magnetic resonance methods for quantifying microsecond-to-millisecond motions in biological macromolecules. *Methods Enzymol.* **339,** 204–238.

Pervushin, K., Riek, R., Wider, G., and Wuthrich, K. (1997). Attenuated T2 relaxation by mutual cancellation of dipole-dipole coupling and chemical shift anisotropy indicates an avenue to NMR structures of very large biological macromolecules in solution. *Proc. Natl. Acad. Sci. USA* **94,** 12366–12371.

Prestegard, J. H. (1998). New techniques in structural NMR—anisotropic interactions. *Nat. Struct. Biol.* **5**(Suppl.), 517–522.

Preston, A., Maxim, E., Toland, E., Pishko, E. J., Harvill, E. T., Caroff, M., and Maskell, D. J. (2003). Bordetella bronchiseptica PagP is a Bvg-regulated lipid A palmitoyl transferase that is required for persistent colonization of the mouse respiratory tract. *Mol. Microbiol.* **48,** 725–736.

Robey, M., O'Connell, W., and Cianciotto, N. P. (2001). Identification of Legionella pneumophila rcp, a pagP-like gene that confers resistance to cationic antimicrobial peptides and promotes intracellular infection. *Infect. Immun.* **69,** 4276–4286.

Salzmann, M., Pervushin, K., Wider, G., Senn, H., and Wuthrich, K. (1998). TROSY in triple-resonance experiments: New perspectives for sequential NMR assignment of large proteins. *Proc. Natl. Acad. Sci. USA* **95,** 13585–13590.

Sass, H. J., Musco, G., Stahl, S. J., Wingfield, P. T., and Grzesiek, S. (2000). Solution NMR of proteins within polyacrylamide gels: Diffusional properties and residual alignment by mechanical stress or embedding of oriented purple membranes. *J. Biomol. NMR* **18,** 303–309.

Tamm, L. K., Abildgaard, F., Arora, A., Blad, H., and Bushweller, J. H. (2003). Structure, dynamics and function of the outer membrane protein A (OmpA) and influenza hemagglutinin fusion domain in detergent micelles by solution NMR. *FEBS Lett.* **555,** 139–143.

Tjandra, N., and Bax, A. (1997). Direct measurement of distances and angles in biomolecules by NMR in a dilute liquid crystalline medium. *Science* **278,** 1111–1114.

Tollinger, M., Skrynnikov, N. R., Mulder, F. A., Forman-Kay, J. D., and Kay, L. E. (2001). Slow dynamics in folded and unfolded states of an SH3 domain. *J. Am. Chem. Soc.* **123,** 11341–11352.

Tugarinov, V., and Kay, L. E. (2003). Ile, Leu, and Val methyl assignments of the 723-residue malate synthase G using a new labeling strategy and novel NMR methods. *J. Am. Chem. Soc.* **125,** 13868–13878.

Tugarinov, V., Hwang, P. M., Ollerenshaw, J. E., and Kay, L. E. (2003). Cross-correlated relaxation enhanced H-1-C-13 NMR spectroscopy of methyl groups in very high molecular weight proteins and protein complexes. *J. Am. Chem. Soc.* **125,** 10420–10428.

Wishart, D. S., and Case, D. A. (2001). Use of chemical shifts in macromolecular structure determination. *Methods Enzymol.* **338,** 3–34.
Yang, D. W., and Kay, L. E. (1999). TROSY triple-resonance four-dimensional NMR spectroscopy of a 46 ns tumbling protein. *J. Am. Chem. Soc.* **121,** 2571–2575.
Yang, D. W., and Nagayama, K. (1996). A sensitivity-enhanced method for measuring heteronuclear long-range coupling constants from the displacement of signals in two 1D subspectra. *J. Magn. Reson. Ser. A* **118,** 117–121.

[14] NMR Experiments on Aligned Samples of Membrane Proteins

By A. A. De Angelis, D. H. Jones, C. V. Grant, S. H. Park, M. F. Mesleh, and S. J. Opella

Abstract

NMR methods can be used to determine the structures of membrane proteins. Lipids can be chosen so that protein-containing micelles, bicelles, or bilayers are available as samples. All three types of samples can be aligned weakly or strongly, depending on their rotational correlation time. Solution NMR methods can be used with weakly aligned micelle and small bicelle samples. Solid-state NMR methods can be used with mechanically aligned bilayer and magnetically aligned bicelle samples.

Introduction

Membrane proteins are important targets for structure determination. They play key roles in signaling and function as receptors for small molecules and their surrogates that act as drugs. There are two major classes of membrane proteins. The three-dimensional structures of several examples of β-barrel membrane proteins have been determined by solution nuclear magnetic resonance (NMR) spectroscopy (Fernandez *et al*., 2004; Hwang *et al*., 2002) and X-ray crystallography (Schulz, 2002). However, the vast majority of membrane proteins are helical (White and Wimley, 1999), and only a small fraction of these have had their structures determined (White, 2004). NMR spectroscopy is emerging as a method capable of determining the atomic-resolution structures of helical membrane proteins in lipid environments that enable them to maintain their native structures and functions.

There are several different NMR approaches to structure determination of helical membrane proteins (Auger, 2000; de Groot, 2000; Drechsler

0076-6879/05 $35.00